Vol 14 No 7, July 2005
1009-1963/2005/14(07)/1457-08

Chinese Physics

© 2005 Chin. Phys. Soc.
and IOP Publishing Ltd

Investigation of the a-Si:H films by using thermal and light-induced annealing treatment in atomic hydrogen atmosphere in H-W-ECR CVD system*

Hu Yue-Hui(胡跃辉)[a)b)], Zhu Xiu-Hong(朱秀红)[a)], Chen Guang-Hua(陈光华)[a)†], Rong Yan-Dong(荣延栋)[a)], Li Ying(李 瀛)[a)], Song Xue-Mei(宋雪梅)[a)], Zhou Huai-En(周怀恩)[a)], Gao Zhuo(高 卓)[a)], Ma Zhan-Jie(马占杰)[a)], and Deng Jin-Xiang(邓金祥)[a)]

[a)] *Department of Material Science and Engineering, Beijing University of Technology, Beijing* 100022, *China*

[b)] *Jingdezhen Ceramic Institute, Jingdezhen* 333001, *China*

(Received 15 October 2004; revised manuscript received 2 March 2005)

To Investigate the stability of hydrogenated amorphous silicon (a-Si:H) films, the thermal and light-induced annealing treatment in an atomic hydrogen atmosphere (TLAH) is carried out by using a new hot-wire-assisted microwave electron-cyclotron-resonance chemical vapour deposition system (H-W-ECR CVD) modified from a conventional microwave electronic cyclotron resonance chemical vapor deposition system (MWECR CVD). In order to compare with the TLAH method, the experiments of thermal annealing, and thermal and light-induced annealing are also performed. Meanwhile, for the purpose of analysing the photoconductivity degradation quantitative, the photoconductivity degradation is assumed to obey the extended exponential law: $1/\sigma_{\rm ph}=1/\sigma_{\rm s}$-$(1/\sigma_{\rm s}$-$1/\sigma_0)\exp[-(t/\tau)^{\beta}]$, where the extended exponential β and the time constant τ are gained by the slope and the intercept of the line according to the linear relationship between $\ln\left(-\ln\left(\dfrac{\sigma_{\rm s}^{-1}-\sigma_{\rm ph}^{-1}}{\sigma_{\rm s}^{-1}-\sigma_0^{-1}}\right)\right)$ and $\ln t$, deduced from the extended exponential law; the photoconductivity saturation value $\sigma_{\rm s}$ can be obtained by Gaussian fitting according to the relationship between photoconductivity and light-soaking time in the logarithmic coordinate system. The experimental results show that the TLAH can improve the stability, microstructure and opto-electronic properties of the annealed a-Si:H films, obviously decrease their optical band gaps, and remarkably move their photoluminescence spectrum (PL) peaks toward low energies.

Keywords: stability of a-Si:H thin film, TLAH, extended exponential law
PACC: 7865P, 8140E, 8115H

1. Introduction

Light-induced metastable defects or, in other words, the Staebler–Wronski effect can restrict the efficiency of the photonic devices made from a-Si:H and related alloys that are used as inexpensive semiconductor materials. So it is important to study the stability of a-Si:H. At present, using methods such as thermal annealing and light-induced annealing to study the stability of the treated a-Si:H has attracted more and more investigators' interest and become a hot subject,[1−6] which empowers people to further understand the relationship between annealing and metastable defects.

It has been suggested that the creation and removal of metastable dangling bonds in a-Si:H could be driven by heat, light or charge carriers.[7] For this purpose, an experiment to investigate the stability of a-Si:H films by the thermal and light-induced annealing treatment in an atomic hydrogen atmosphere (TLAH) in high vacuum is designed by using a new H-W-ECR CVD system modified from a conventional microwave electronic cyclotron resonance chemical vapour deposition (MWECR CVD) system. In this new system, the auxiliary hot wire has two functions: one is that

*Project supported by the State Key Development Program for Basic Research of China (Grant No 2000028201) and the Jiangxi Province Foundation of China (Grant No 0412023).

†Corresponding author. E-mail: ghchen@bjut.edu.cn

when a-Si:H films are deposited with the aid of the hot wire at high temperatures, radical species produced by decomposing silane in an electronic cyclotron resonance (ECR) plasma can be decomposed completely or, in other words, the catalyst is produced which is helpful to further increase their activation, so that device-grade a-Si:H films can be obtained hopefully; the other is that using the strong light radiation produced by the hot filament at high temperatures can also realize light-induced annealing. Vikram *et al*[8] have fabricated device-grade a-Si:H films, which is based on the first function of the hot wire mentioned above. Instead, we use these two functions simultaneously to fabricate a-Si:H films and realize thermal and light-induced annealing (TLA) and TLAH. As a result, we find that their synergistic function is very effective.

2. Experiment

Based on a conventional ECR CVD system, a new hot-wire-assisted microwave electron-cyclotron-resonance (H-W-ECR) CVD system is designed, as shown in Fig.1; a 120mm diameter tungsten filament ring made of a 0.5mm diameter is located above 80mm away from the sample stage to ensure the minimized radiative heat to the substrate, and connected with an AC transformer on both sides with a voltage of 10.6V, corresponding to a light intensity of 80.4mW/cm^2 emitted from the hot filament. The deposition condition of a-Si:H films is shown in Table 1. Substrates (glass and Si wafer) are rinsed and soaked in eluent in order to remove the metal ions, then the grease on the substrates is removed respectively in toluene, acetone, and ethanol, and finally they are soaked in ethanol to be kept in reserve. When used in experiment, they are picked out from the ethanol, and then dried, and finally located on the substrate holder. The hot wire is treated by 13.6V for 3 minutes before deposition. A ceramic DC heat furnace, which is capable of controlling the temperature precisely, is used to heat the substrates. For the measuring of infrared transmission spectroscopy, the films are prepared on the double-side polished Si wafer and measured by Xian-Chinetek FTIR 1020 Fourier spectrometers. For the measuring of photoconductivity, dark conductivity, optical band gap, PL spectrum and Urbach energy E_0, the films are prepared on the glass. The photoconductivity and dark conductivity are measured by using the Keithley 6517 Electrometer/High Resistance System. Evaporated coplanar aluminium electrodes with a separation of 1mm are used for measuring the conductivity. The photoconductivity is measured under simulated AM1 (100mW/cm^2) illumination. The Urbach energy E_0 is obtained by using photoconductivity spectroscopy techniques.[9] Light absorption and reflection data in the SHIMADZU-3101PC range of photon energy are taken from the UV–VIS–NIR scanning spectrophotometer, and the optical gaps of thin films are determined by use of Tauc's method. PL spectra are obtained by using the RENISHAW (RM2000) spectrophotometer with a 1.0cm^{-1} resolution and a 2.3mW Ar^+ laser with an excitation wavelength of 514.5nm at room temperature.

Table 1. Deposition condition of a-Si:H films.

Background pressure	8.5×10^{-4}Pa
Flux of hydrogen-diluted silane (SiH_4 / (SiH_4+ H_2)=20%)	25sccm
Deposition pressure	0.8Pa
Substrate temperature	240°C
Microwave power	480W
Distance from hot wire to substrate	80mm
Hot wire temperature	1600°C (Corresponding to 10.6V AC voltage)
Substrate	glass, single crystal silicon wafer
Distance from substrate to microwave window	130mm
Deposition time	9 min (about 0.8μm thick)

The heater, as shown in Fig.1, determines the annealing temperature. The strong light emission coming from the tungsten filament heated up to a high temperature is used for light-induced annealing. 0#, 1#, 2# and 3# are used to number the four deposited samples. Of them, the sample 0# is as-deposited and the samples 1#, 2# and 3# are annealed in the deposition chamber pumped down to 4.5×10^{-4}Pa. The annealing condition of samples is shown in Table 2. On the same condition that annealing time is 90 min-

utes and the samples are heated up to a temperature of 200°C, the three samples are annealed in different ways. For sample 1#, the thermal and light-induced annealing is used with a voltage of 10.6V applied to the hot wire; correspondingly, the light intensity 80.4 mW/cm^2 is achieved by strong light emission from the tungsten filament at a high temperature. For sample 2#, its annealing is performed under the same condition as that of the sample 1#, except for hydrogen with a 20 sccm flux being used in the annealing process. For sample 3#, only thermal annealing is conducted.

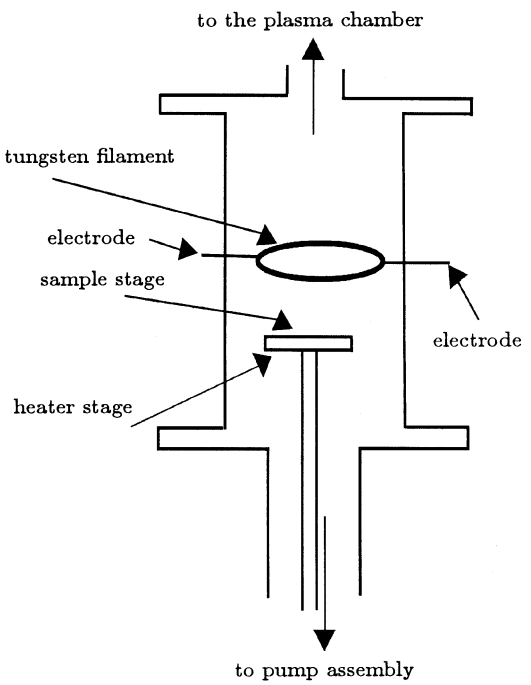


Fig.1. Schematic diagram of the H-W-MWECR CVD system modified from a conventional MWECR CVD.

Table 2. Annealing condition of samples.

Sample No	Annealing condition
0#	As-deposited
1#	Thermal and light-induced annealing at 200°C.
2#	Thermal and light-induced annealing at 200°C in an atomic hydrogen atmosphere with a 20 sccm flux
3#	Only thermal annealing at 200°C

Note: annealing time is 90 minutes; the light intensity produced by the tungsten filament with a applied voltage of 10.6 V is 80.4mW/cm^2

3. Results and discussion

The degradation curves of the photoconductivity of these samples are shown in Fig.2(a). Figure 2(b) is replotted from Fig.2(a) according to the relation between photoconductivity and light-soaking time in the logarithmic coordinate system. It is shown that there is remarkable difference in photoconductivity degradation between the samples treated using the light-induced annealing method (such as TLA and TLAH) and the samples treated using other annealing methods (such as TA and as-deposited). For the 1# and 2# samples, their photoconductivity reduces slowly with ln$t$ at the beginning of light soaking, then almost linearly with ln$t$. But for the 0# and 3# samples, their photoconductivity degradation is obviously linear at the beginning.

The quantitative results of photoconductivity degradation can be obtained using the extended exponential law of light-induced metastable defect density:

$$N(t) = N(\infty) - (N(\infty) - N(0))\mathrm{e}^{[-(t/\tau)^{\beta}]},$$

where τ is the time constant, and β is the parameter of extended exponential. When illumination intensity is strong enough, $\sigma_{\mathrm{ph}} \propto 1/N(t)$.[10] Using the extended exponential law, the result of photoconductivity degradation can be expressed as

$$\frac{1}{\sigma_{\mathrm{ph}}} = \frac{1}{\sigma_{\mathrm{s}}} - \left(\frac{1}{\sigma_{\mathrm{s}}} - \frac{1}{\sigma_0}\right)\mathrm{e}^{[-(t/\tau)^{\beta}]}. \qquad (1)$$

where σ_{ph} denotes photoconductivity, σ_{s} is the saturation value of σ_{ph} and σ_0 is the primary value of σ_{ph}. Obviously, the bigger the value of τ or the smaller the value of β is, the more slowly the photoconductivity degrades. In order to obtain the values of τ and β, Eq.(2) is deduced from Eq.(1), and expressed as

$$\beta \ln t - \beta \ln \tau = \ln\left(-\ln\left(\frac{\sigma_{\mathrm{s}}^{-1} - \sigma_{\mathrm{ph}}^{-1}}{\sigma_{\mathrm{s}}^{-1} - \sigma_0^{-1}}\right)\right), \qquad (2)$$

where σ_{s} can be obtained by inserting the simulation light-soaking time for long enough illumination into the formulae (A0), (A1), (A2) and (A3) in the Appendix for the 0#, 1#, 2# and 3# samples respectively. According to the relationship between $\ln\left(-\ln\left(\frac{\sigma_{\mathrm{s}}^{-1} - \sigma_{\mathrm{ph}}^{-1}}{\sigma_{\mathrm{s}}^{-1} - \sigma_0^{-1}}\right)\right)$ and ln$t$, Fig.2(c) is replotted from Fig.2(b), in which the values of β and τ are obtained from the slope and intercept of the line, as shown in Table 3. The photoconductivity degradation obeys the extend exponential law for the four samples, as shown in Fig.2(c).

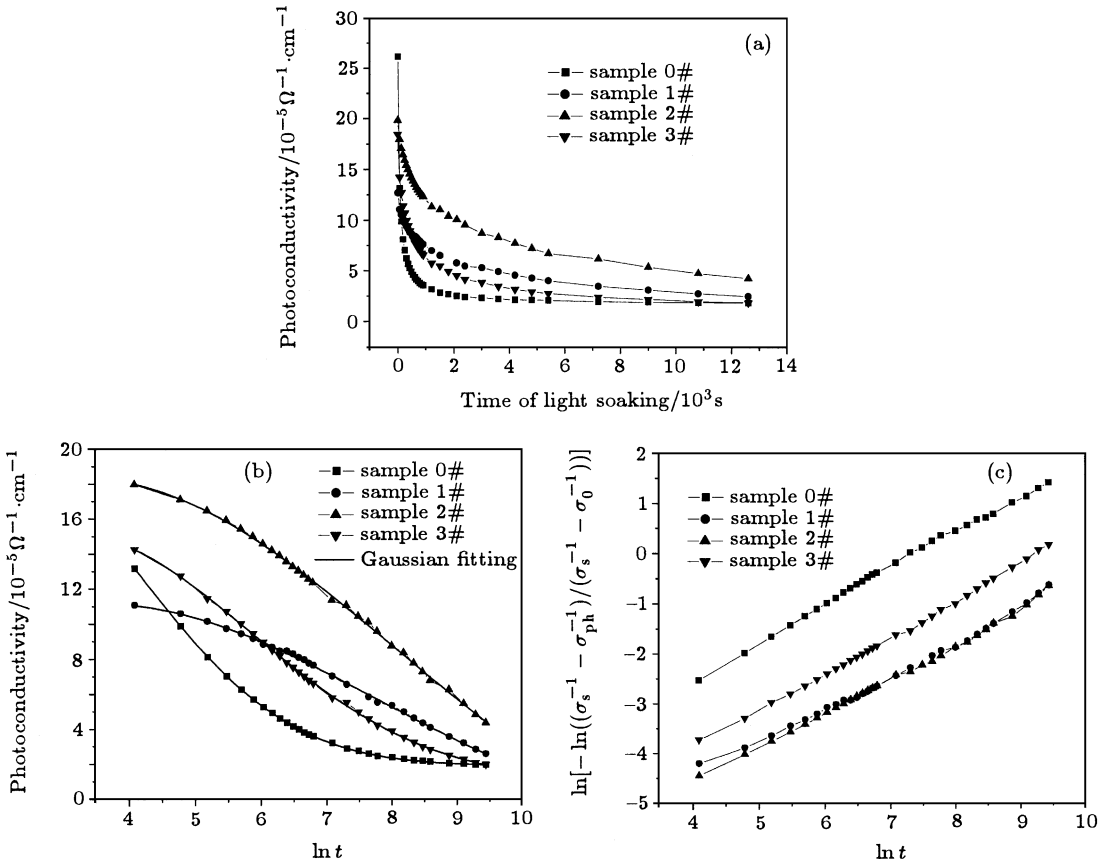


Fig.2. Light-induced change of photoconductivity of a-Si:H films. (a) Relationship between photoconductivity and light-soaking time in the Cartesian coordinate system. (b) Reproduction of Fig.2(a) in the logarithmic coordinate system. (c) Reproduction of Fig.2(b) in the double logarithmic coordinate system from Eq.(2).

The results indicate that the 1# and 2# samples treated respectively by TLA and TLAH exhibit higher stability (β is smaller and τ is bigger).

Table 3. The result of photoconductivity degradation.

Samples	$\sigma_0/(\Omega^{-1}\cdot cm^{-1})$	$\sigma_s/(\Omega^{-1}\cdot cm^{-1})$	β	τ	Time of light-soaking/s	Time of simulation light-soaking/s
0#	2.62×10^{-4}	1.88×10^{-5}	0.72	1635.96		
1#	1.27×10^{-4}	1.17×10^{-5}	0.67	45206.67	12600	30000
2#	1.98×10^{-4}	1.98×10^{-5}	0.69	31194.59		
3#	1.85×10^{-4}	1.37×10^{-5}	0.73	11292.56		

The hydrogen diffusion-controlled defect bond relaxation model (HCR)[11] can explain this result. In a-Si:H thin films, energy is released during electron–hole pair recombination, and hydrogen atoms are excited into mobile states. The metastable defects are produced when the hydrogen atoms diffuse near a weak Si–Si bond (defect resource) and are trapped there. Based on this model, the factor influencing the generation of metastable defect is the dispersive diffusion of hydrogen, which takes place on the lattices of traps distributed exponentially. In the light-induced annealing process, structural rearrangements of atoms caused by electronic transitions during light soaking result in generating many inhomogeneities in the form of void and microvoids in the network to release their stresses, which can form a rigid network structure.[12] In this way, a defect source with a high barrier is formed, and hydrogen atoms have to overcome this high barrier to generate defects. As a result, on the one hand, this leads to τ increasing, on the other hand, this results in the increase in dispersive diffusion of hydrogen atoms, i.e. the decrease in β.

Table 4. The physical properties and structure parameters of samples.

Samples	E_0/meV	C_H/(at%)	F	E_g/eV	σ_{ph}/σ_d
0#	66.68	15.99	4.11	1,76	2.9×10^5
1#	70.11	15.71	3.46	1.71	5.6×10^3
2#	68.97	15.48	5.96	1.65	2.4×10^4
3#	66.28	15.78	6.68	1.72	8.6×10^4

As shown in Table 4, the widths of band tail E_0 have become broad obviously for the 1# and 2# samples, which indicates that the dangling bond density increases under the condition of light-induced annealing. But for the 2# sample the width of band tail is narrow compared with that for the 1# sample (reduced by about 1.2meV), which implies that the TLAH can reduce the defect remarkably.

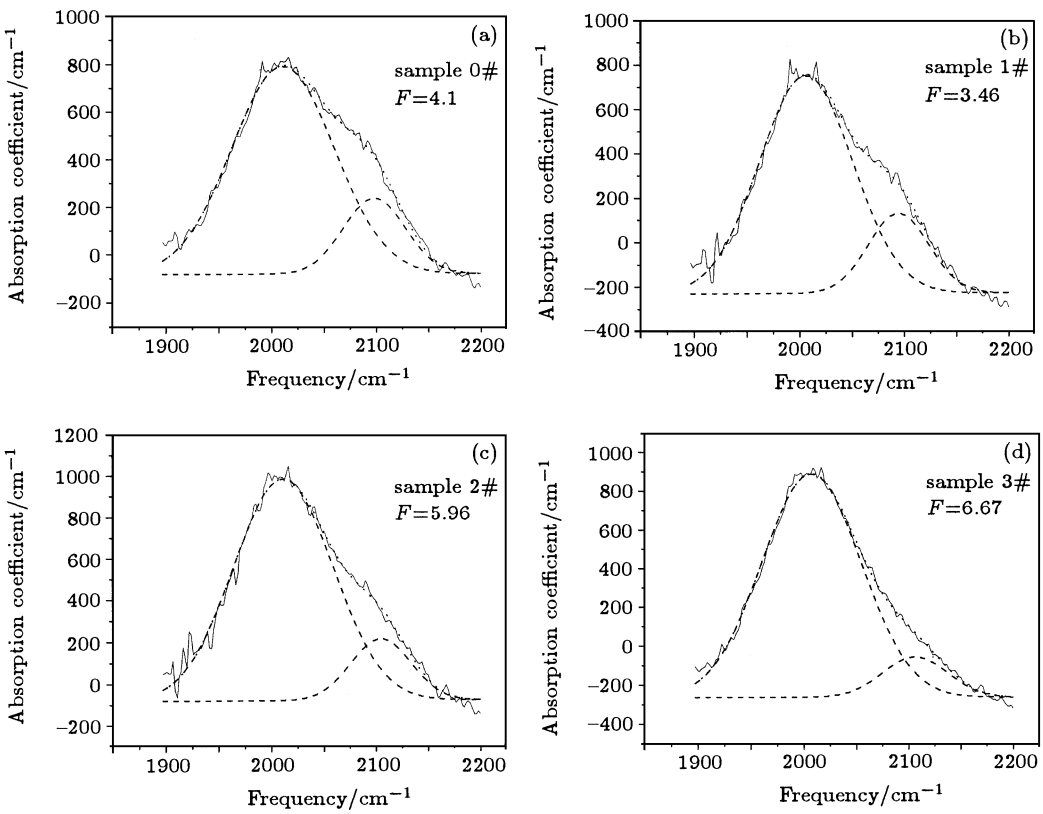


Fig.3. Stretching modes of infrared absorption spectra: (a) as-deposited sample; (b) thermal and light-induced annealing at 200°C; (c) thermal and light-induced annealing treatment in an atomic hydrogen atmosphere at 200°C; (d) only thermal annealing at 200°C. The content of monohydride (SiH) is indicated in terms of a structure factor $F = I_{2000}/I_{2100}$. Solid line: experimental data; dots: fitting curves of double-peaks; dashes: two peaks of monohydride and polyhydride stretching modes at 2000cm^{-1} and 2100cm^{-1}, respectively.

For the samples annealed in different ways, hydrogen content (C_H), which is derived from the infrared-absorption spectra using the stretching modes at around 2000 and 2100cm^{-1}, is observed to have no remarkable change. Considering the base line fitting and the other factors affecting the reliability of calculating hydrogen content,[13] we calculate the integrated intensities of the stretching band peaked at around 2000 and 2100cm^{-1} of I_{2000} and I_{2100} which correspond to monohydride and polyhydride (including clustered monohydride) respectively.[14] The results show that the structure factors F ($F = I_{2000}/I_{2100}$) of the samples annealed in different ways are obviously different. Of them, the structure factor of the 1# sample is the smallest, which implies that the monohydride content decreases remarkably. It is notable that the structure factor of the 2# sample increases obviously, which suggests that silicon-hydrogen bond configuration can be improved by use of TLAH method. The silicon–hydrogen bond configurations of samples are shown in Fig.3.

Although the difference in total hydrogen content between the samples annealed in different ways is not remarkable, the silicon–hydrogen bond configuration of the sample treated in a hydrogen atmosphere in the process of light-induced annealing can be im-

proved obviously. The reason is that atomic hydrogen is a strong chemical agent, which has a high chemical potential and extremely small physical dimension. It is thought that during annealing, hydrogen atoms penetrate the a-Si:H and selectively attack the defects in the network-like voids, microvoids as well as the weakly bonded polyhydride, due to a strong chemical affinity and the excess hydrogen atoms evolving out of the solid phase in the form of gaseous molecular structure with a lower free energy.[12] Therefore, in the process of TLAH, atomic hydrogen plays a significant role in reconstructing the Si-network and controlling the hydrogen content in the bulk.[15]

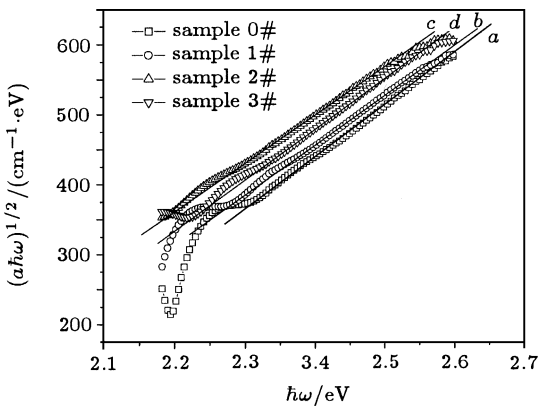


Fig.4. Tauc plot of the samples annealed in different ways. The optical band gap of samples 0#, 1#, 2# and 3# are of 1.76eV, 1.71eV, 1.65eV and 1.72eV, respectively, deduced from the intercept of lines *a*, *b*, *c* and *d*.

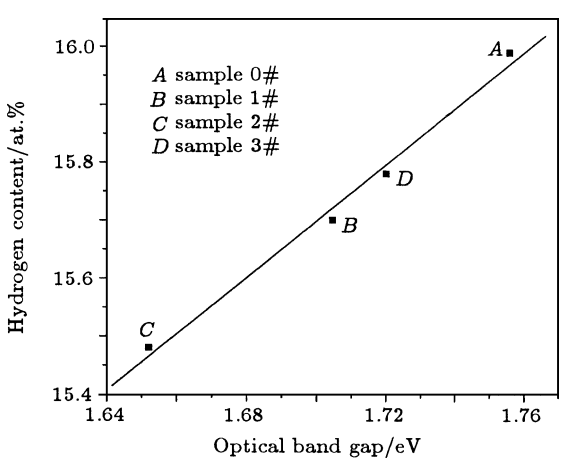


Fig.5. Relationship between optical band gap and hydrogen content.

Figure 4 shows the optical band gaps of samples annealed in different ways, and Fig.5 indicates the corresponding relationship between the optical band gap and the hydrogen content. It is notable that the 2# sample possesses the narrowest band gap, which may be owing to the rigid network structure of the a-Si:H film treated with TLAH. The relationship between optical band gap and hydrogen content is linear, which is consistent with that in the reference [16].

As shown in Fig.6, it is interesting that the 2# sample has a remarkably low PL peak compared with other samples. It is because the 2# sample has the smallest optical band gap. Using the as-deposited sample (0# sample) as a reference, the relationships between PL peak shift and the change of band gap for the three samples annealed by different ways are shown in Fig.7. It can be seen that the PL peaks shift toward the low energies as optical band gap becomes narrow, which is consistent with the result in Ref.[17].

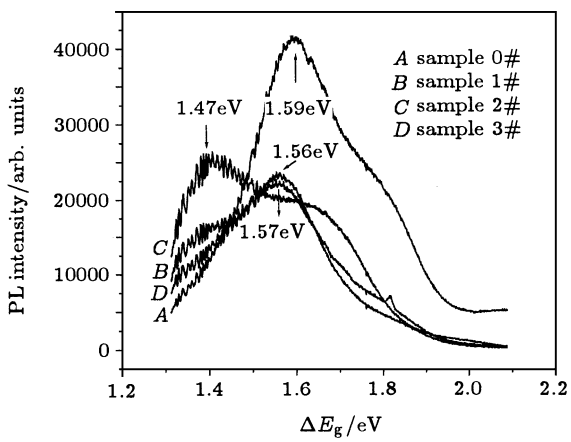


Fig.6. Photoluminescence spectra of the samples annealed in different ways.

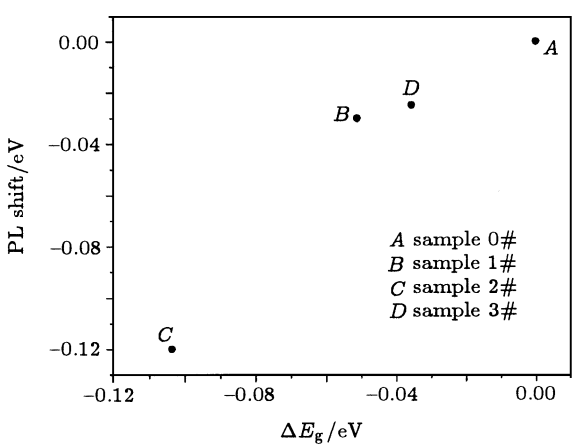


Fig.7. Relationship between ΔE_g and PL shift after annealing, where ΔE_g is the change of the optical band gap relative to that of the as-deposited sample, and PL shift is a shift relative to that of the as-deposited sample.

As shown in Table 4, the photosensitivity is more complex. It is determined by the ratio of photoconductivity to dark conductivity σ_{ph}/σ_d, where σ_{ph} is

determined by hydrogen bond configuration, optical gap and short range order; σ_d is related to the surface roughness. Although the structure factor F of the 3# sample is bigger than that of the 0# sample, which implies that the 3# sample has a better hydrogen bond configuration, the thermal annealing may lead to the reduction in the surface roughness[18] under the proper condition, as a result σ_d increases, and σ_{ph}/σ_d of the 3# sample may be smaller than that of the 0# sample. It is noteworthy that the photosensitivity of the sample 1# becomes worse remarkably, while for the sample 2#, its photosensitivity is improved up to 2.4×10^4. This phenomenon should be attributed to the significant role played by hydrogen atoms in improving hydrogen bond configuration under the same condition of thermal and light-induced annealing.

4. Conclusion

The light-induced annealing is realized by using an H-W-ECR CVD system. Although the photoconductivity degradation of the samples annealed in different ways is in good agreement with the extended exponential relation, there exists remarkable difference in the decay behaviour between the samples treated using light-induced annealing method and those using other annealing methods. The saturation value of photoconductivity can be obtained by inserting the simulation light-soaking time which is considered long enough for illuminance into the formulas (A0), (A1), (A2) and (A3) for the 0#, 1#, 2# and 3# samples, respectively, as indicated in the Appendix. Consequently, according to the relationship between $\ln\left(-\ln\left(\frac{\sigma_s^{-1}-\sigma_{ph}^{-1}}{\sigma_s^{-1}-\sigma_0^{-1}}\right)\right)$ and $\ln t$, the β and τ can be obtained easily in the logarithmic coordinate system. The experimental results show that the TLAH method can improve the stability, microstructure and optoelectronic properties of the annealed a-Si:H films, obviously decrease the optical band gaps, and remarkably move the photoluminescence spectrum peaks toward the low energies.

Appendix

Gaussian equation fitting:

$$y = y_0 + \frac{A}{w\sqrt{\frac{\pi}{2}}} e^{-\frac{2(x-x_0)^2}{w^2}},$$

where

y_0 baseline offset

A total area under the curve from the baseline

x_0 centre of the peak

w 2 "sigma", approximately 0.849 times the width of the peak at half height.

For the Gaussian fitting of four samples in the logarithmic coordinate system, the relationship between photoconductivity and light-soaking time is shown in Fig.2(b), and their fitting parameters are shown in Table A-1:

Table A-1. The Gaussian fitting parameters of four samples.

Samples number	Fitting parameters			
	y_0	A	x_0	w
0#	1.8576×10^{-5}	0.0010250	1.9027	4.5116
1#	-2.6839×10^{-5}	0.0014782	3.5016	8.4996
2#	-6.7848×10^{-5}	0.0030884	3.2024	9.7755
3#	9.0626×10^{-6}	9.9666×10^{-4}	3.0462	5.5455

Inserting the fitting parameters into the Gaussian equation fitting and using the logarithmic coordinate system in Fig.2(b), the formulae of photoconductivity for the 0#, 1#, 2# and 3# samples are given as follows:

$$\sigma_{ph} = 0.000018576 + 0.0001813e^{-0.09826(\ln t - 1.9027)^2}, \quad (A0)$$

$$\sigma_{ph} = -0.000026839 + 0.0001388e^{-0.02768(\ln t - 3.5016)^2}, \quad (A1)$$

$$\sigma_{ph} = -0.000067848 + 0.00025214e^{-0.020929(\ln t - 3.204)^2}, \quad (A2)$$

$$\sigma_{ph} = 0.0000090626 + 0.000143435e^{-0.065035(\ln t - 3.0462)^2}. \quad (A3)$$

References

[1] Alp O K 2002 *Mater. Sci. Eng.* B **95** 67

[2] Wang L, Huang X, Ma Z and Li Z 2002 *Appl. Phys.* A **74** 783

[3] Serin T, Serin N, Tarimci C and Ünal B 2000 *J. Non-Cryst. Solids* **276** 163

[4] Xin Y, Ning Z Y, Cheng S H, Lu X H, Gan Z Q and Huang S 2002 *Acta Phys. Sin.* **51** 439 (in Chinese)

[5] Takeda K, Hikita H, Kimura Y and Yokomichi H 1996 *J.*

Non-Cryst. Solids **198–200** 486
[6] Pivac B *et al* 2003 *Vacuum* **71** 135
[7] Gleskova H and Wagner S 1995 *J. Non-Cryst. Solids* **190** 157
[8] Vikram L D, Paul S and Matt R 2003 *Thin Solid Films* **430** 91
[9] Datta T, Woollam John A and Notohamiprodjo W 1989 *Phys. Rev.* B **40** 5956
[10] Dalal V L and Fulenhan C 1989 *Mat. Res. Symp. Proc.* **149** 601
[11] Kakalios J Street R A and Jackson W B 1987 *Phys. Rev. Lett.* **59** 1037
[12] Das D 2004 *Solar Energy Mater. Solar Cells* **81** 155
[13] Hu Y H, Chen G H and Wu Y Y 2004 *Sci. Chin.* G **31** 234
[14] Manfredotti C, Fizzotti F and Boero M 1994 *Phys. Rev.* B **50** 18046
[15] Das D 1995 *Phys. Rev.* B **51** 10729
[16] Copy G D and Wronski C R 1980 *Solar Cells* **2** 227
[17] Chen Z 1983 *Phys.* **3** 180
[18] Kang M 1996 *IEEE Proceedings International Conference on Optoelectronic and Microelectronic Materials and Devices Proceedings* (Australia) p483